CHEMISTRY

Nonlinear infrared polaritonic interaction between cavities mediated by molecular vibrations at ultrafast time scale

Bo Xiang[1], Jiaxi Wang[2], Zimo Yang[1], Wei Xiong[1,2]*

Realizing nonlinear interactions between spatially separated particles can advance molecular science and technology, including remote catalysis of chemical reactions, ultrafast processing of information in infrared (IR) photonic circuitry, and advanced platforms for quantum simulations with increased complexity. Here, we achieved nonlinear interactions at ultrafast time scale between polaritons contained in spatially adjacent cavities in the mid-IR regime, altering polaritons in one cavity by pumping polaritons in an adjacent one. This was done by strong coupling molecular vibrational modes with photon modes, a process that combines characteristics of both photon delocalization and molecular nonlinearity. The dual photon/molecule character of polaritons enables delocalized nonlinearity—a property that neither molecular nor cavity mode would have alone.

INTRODUCTION

Nonlinear interactions between molecular vibrational modes, referred as molecular vibrational nonlinearity hereafter, are crucial to distribute energies among chemical groups during reactions. However, they are localized within Angstroms due to the physical dimensions of molecular potential energy surfaces, e.g., Morse or double well potentials. Even intermolecular nonlinear interactions through dipole-dipole interactions are limited to a few nanometers. Because the molecular vibrational nonlinearity is localized, the reactants have to be close to each other in liquid phase to react, making many reactions limited by diffusions. Being able to delocalize nonlinear interactions across micron-length distances thus has the potential to trigger certain reactions without the reactants being spaced closely. Meanwhile, nonlinear interactions of photons are the crucial components for photonic circuitry (*1*, *2*), and such interactions in the mid-IR regime can enable chemical sensing in the molecular fingerprints region. However, scaling up of these developments is prohibited, because nonlinear infrared (IR) interactions mediated by molecules are localized. Thus, delocalized nonlinear interactions in the IR regime could be critical for future photonic applications.

In this work, we report nonlinearity between polaritons in two adjacent cavities. By exciting polaritons in one cavity, we affect polaritons in the neighboring cavity whose geometric centers are tens of microns away, through strong coupling between the vibrational and cavity modes (*3*–*13*). The strong coupling between molecular vibrational and cavity modes forms molecular vibrational polaritons, which has enabled exotic phenomena such as vibrational energy transfer between molecules in the liquid phase (*14*), and modified chemical reaction selectivity (*15*). In polariton systems, the molecular vibrational anharmonicity provides local sources of optical nonlinearity, while photon cavity modes are macroscopic and delocalized but linear. The strong light-matter coupling then combines photon delocalization with molecular nonlinearity, which otherwise would not exist in either mode alone. We note that the idea of combining material nonlinearity with hybridized cavities was first proposed in atomic-molecular physics for quantum simulation (*16*) and recently demonstrated in inorganic semiconductor exciton-polaritons (*17*, *18*). The present work enables intercavity nonlinearity with liquid phase molecular systems and directly time resolve its dynamics. We refer to this nonlinearity as intercavity polariton nonlinear interactions.

RESULTS

To realize intercavity polariton nonlinear interactions, we fabricate a coupled Fabry-Perot (FP) cavity and conduct linear and nonlinear IR spectroscopy on coupled cavity polaritons. A checkerboard matrix is composed of individual FP cavities, where cavities with two thicknesses (12.50 and 12.69 μm for cavities A and B, respectively; Fig. 1, B and C; see Supplementary Methods), and two distinct transition frequencies (1970 and 2000 cm^{-1}; Fig. 1D), alternate. Here, neighboring cavities can overlap through evanescent waves along the transverse directions, and the molecular modes in the overlapping volumes should enable nonlinear interactions (*4*, *7*, *8*) between polaritons in adjacent cavities (Fig. 1A). Experimentally, we found that the optimal cavity lateral dimension was 50 μm. We believe that at this size, it ensures a sufficient interaction between neighboring cavities while keeping the two cavity modes distinguishable. Furthermore, because the diameter of IR laser beam is about 100 μm, cavities with 50-μm lateral dimension avoid spatial inhomogeneity among multiple cavities. We prepared the polaritons by encapsulating a saturated $W(CO)_6$/hexane solution (~40 mM) in the coupled cavity (see Supplementary Methods) (*3*, *7*). $W(CO)_6$ has a strong asymmetric vibrational stretch mode at 1983 cm^{-1}, which is ideal for forming polaritons in the IR regime.

The linear IR spectra of polaritons in the coupled cavity show four peaks (Fig. 1E, right), which is unexpected and makes the transfer matrix model (*19*) challenging to capture the results. From a naïve perspective, if one molecular vibrational mode strongly couples to the two-cavity modes simultaneously, then three IR peaks would be expected (see section S3.4 for details), which disagrees with the observed four-peak feature. An alternative model is that the molecular vibrations couple to the two cavities separately, each forming one pair of upper polariton (UP) and lower polariton (LP), i.e., UP1 and LP1 in cavity A and UP2 and LP2 in cavity B, respectively, composing the total four peaks. To test this idea, we prepared

[1]Materials Science and Engineering Program, UC San Diego, La Jolla, CA 92093, USA. [2]Department of Chemistry and Biochemistry, UC San Diego, La Jolla, CA 92093, USA. *Corresponding author. Email: w2xiong@ucsd.edu

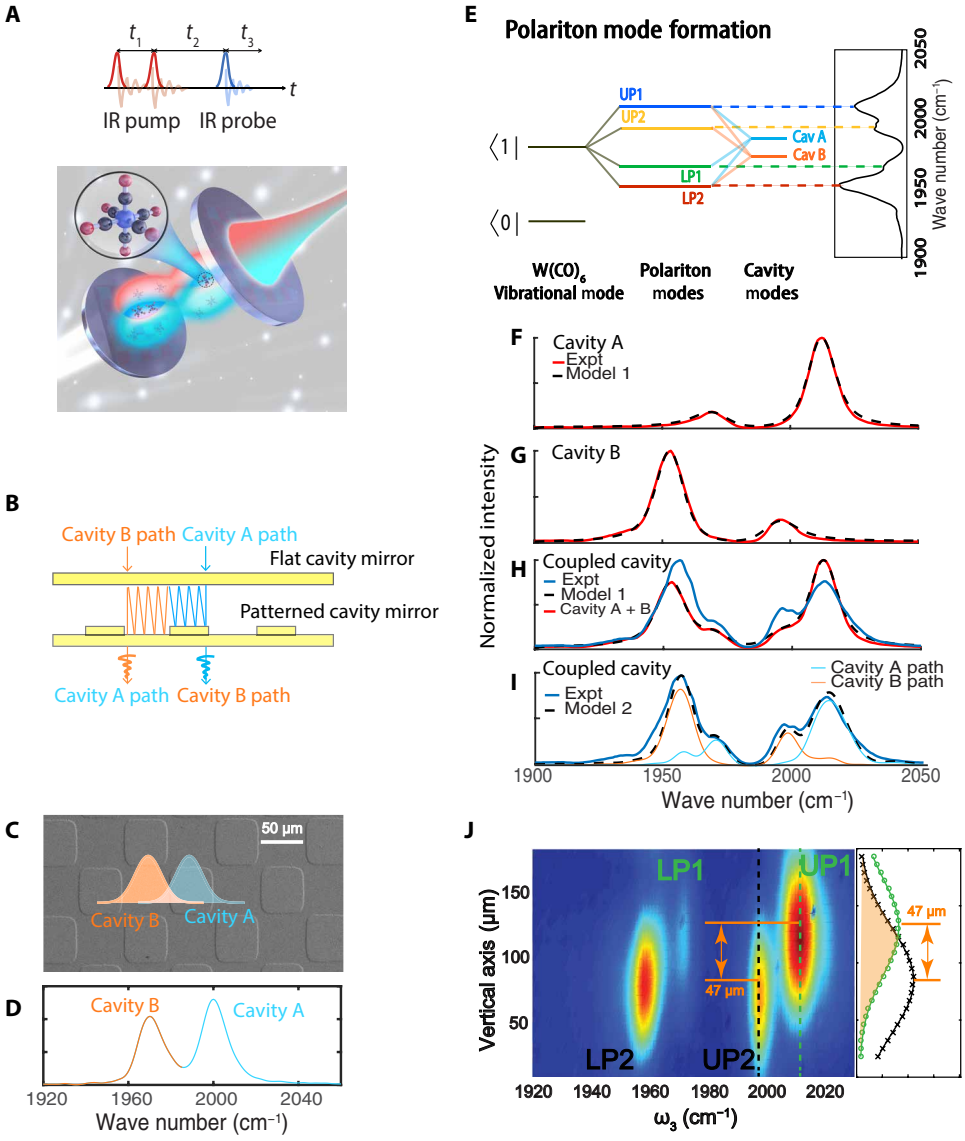

Fig. 1. Key idea of intercavity nonlinear interactions between polaritons. (**A**) Illustration of a coupled cavity and 2D IR pulse sequence. The key to enable intercavity nonlinear interaction is to have anharmonic molecules (enlarged) in the shared volume between cavities. (**B**) A proposed mechanism of coupling between cavities. When a photon enters into cavity A, it hops to cavity B and exits from there (cavity A path). The reversed direction (cavity B path) could happen too. (**C**) Scanning electron microscopy of checkerboard-patterned cavity mirror. (**D**) FTIR of the dual cavity modes (1970 and 2000 cm^{-1}). (**E**) Energy diagram of polariton modes formed by the coupling of $W(CO)_6$ with the coupled cavity. (**F** to **I**) Experimental and simulated linear IR transmission of polaritons. (F and G) Polariton tranmission spectra in a regular cavity detuned to match the resonance of cavities A and B, which can be well fitted by model 1. (H) Experimental polariton tranmission spectra of the coupled cavity and the summed spectra of (F) and (G). (I) Experimental and simulated linear IR of polaritons in the coupled cavity. Using model 2 (see the main text and section S2.2 for details), the experimental spectra can be well simulated. Additional minor polariton peaks appear due to delocalization to the neighboring modes. (**J**) Transmission image of coupled cavity polariton system where LP1/UP1 states (cavity A polaritons) locate at the top part, while the LP2/UP2 states (cavity B polaritons) locate at the bottom part. The spatial separation between cavity A and B polaritons is 47 μm, close to the pattern size of 50 μm. There is a substantial overlapping area between the two modes as a result of mode delocalization, which is highlighted as an orange area on the right panel. See detailed experimental setup in section S3.7.

the two polariton systems, i.e., UP1/LP1 and UP2/LP2, separately, using regular FP cavities (Fig. 1, F and G), measured their corresponding spectra, and then add them together numerically, to mimic the coupled cavity polaritons. The peak positions of the summed spectrum match well with the one of the coupled cavities, but the intensities do not (Fig. 1H). Similarly, while the transfer matrix method (*19*) (model 1, see section S2.1) can simulate polariton spectra of regular FP cavity perfectly (dashed lines in Fig. 1, F and G), it cannot reproduce the spectral intensity of the polaritons in the coupled cavity (dashed lines in Fig. 1H).

The intensity mismatch suggests that a component is missing from the transfer matrix model to account for the intensity redistribution among spectral peaks. We extended the transfer matrix model by including photon hopping [i.e., light lateral transmission via multireflections on the cavity mirror surfaces (*20*)] and show that the missing component is the delocalization of cavity modes:

Upon entering cavity A, photons can hop to cavity B and subsequently interact with molecular vibrations in cavity B, representing the delocalization between cavities (the cavity A path in Fig. 1B). An alternative path also exists (cavity B path in Fig. 1B). The expression of transmission spectra based on the model 2 is summarized in Eq. 1 (detailed derivation in section S2.2).

$$T = \left[\frac{T_1 e^{-\frac{1}{2}\alpha L_1}}{1 - R_1 e^{i\Delta\varphi_1 - \alpha L_1}} (1 - R_1^n e^{-n\alpha L_1 + in\Delta\varphi_1}) + \frac{\sqrt{T_1 T_2}\, e^{-\frac{1}{2}\alpha L_1}}{1 - R_2 e^{i\Delta\varphi_2 - \alpha L_2}} (R_1^{n-1} e^{-(n-1)\alpha L_1 + i(n-1)\Delta\varphi_1} R_2 e^{-\alpha L_2 + i\Delta\varphi_2}) \right]^2 \quad (1)$$

where T_m, R_m, L_m, and $\Delta\varphi_m$ are transmission, reflection, cavity thickness, and phase shift of cavity m, respectively, α is the absorptive coefficient of molecules, and n represents the number of round trips before photon hopping to the adjacent cavity. Results from model 2 reproduced both the peak position and intensities from the experimental measurements (Fig. 1I, detailed model in section S2.3 and fitting parameters in section S3.2). The model 2 result shows that the linear IR spectra are a combination of two sets of polaritons from the cavity A and B paths, respectively (orange and cyan traces in Fig. 1I). Thus, molecular modes in each cavity strongly couple to the cavity mode that they reside in and weakly couple to the adjacent cavity mode (Fig. 1E). We note that the intermolecular interaction is negligible to contribute to the linear IR of coupled cavity polaritons (see section S3.4).

This photon hopping picture is further supported by an IR hyperspectral image of the coupled cavity polaritons (Fig. 1J). This image is composed of a series of spectra of a vertical slice of the coupled cavity polariton image, taken by a focal plane array (FPA) mercury-cadmium-telluride (MCT) detector (detailed description of the setup in section S3.7). Thus, the vertical axis of the image represents the location of the polaritons, and the horizontal axis corresponds to the frequency of the polariton features. We can identify the UP1 and LP1 from cavity A at 116 μm and UP2 and LP2 from cavity B at 69 μm. The two pairs of polaritons are spatially displaced along the vertical by 47 μm, agreeing with the scanning electron microscopy image (Fig. 1C). However, vertical cuts show polaritons in each cavity leak into their neighboring cavity, as the width of polaritons are 59 and 64 μm, larger than the 50-μm dimension of the cavity. This result suggests that cavity mode delocalization exists, which is a critical component for intercavity polariton nonlinear interactions (*16*). However, we have not yet demonstrated that the delocalization leads to nonlinear interactions across cavities, in which excited polaritons influence those in an adjacent cavity, occurred.

To examine intercavity polariton nonlinear interactions, we conduct two-dimensional (2D) IR spectroscopy (*7*, *10*, *21*–*25*). 2D IR measures the third-order nonlinear response of the systems. The pulse sequence described in Fig. 1A excites two vibrational coherences at various time incidences and tracks the interaction and dynamics of quantum states. For example, when two modes interact with each other, e.g., exciting one mode can affect the other mode, cross-peaks appear at the corner defined by the resonance frequencies of the two coupled modes.

2D IR spectra of the coupled cavity polaritons at t_2 = 20 ps show clear cross-peaks (shaded green areas in Fig. 2A). In the following, we perform detailed spectral analysis to show that these cross-peaks are signatures of intercavity polariton nonlinear interactions. On

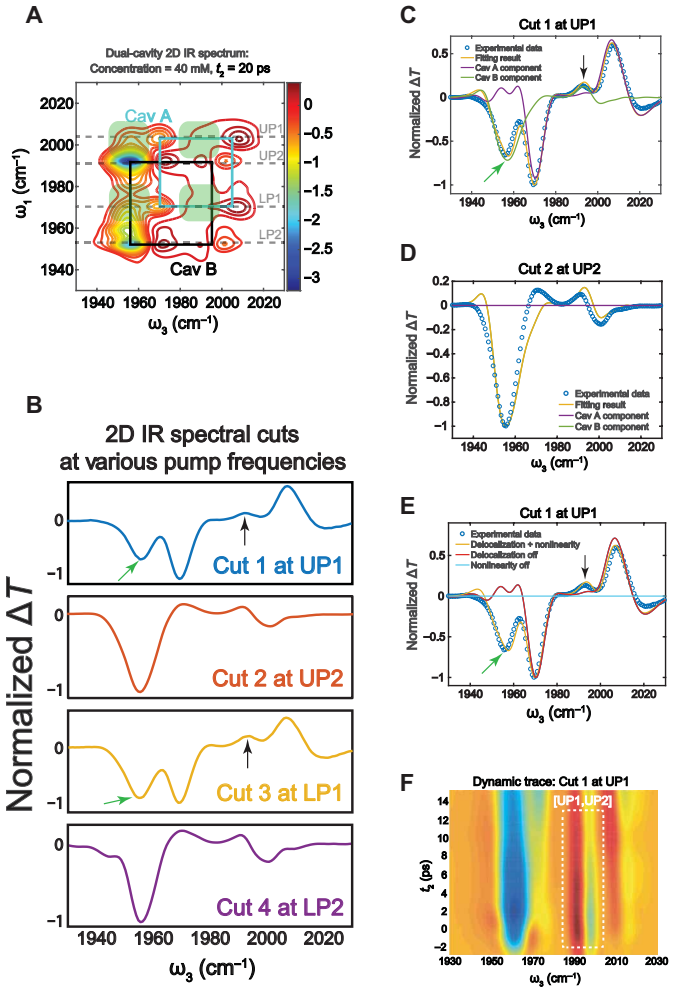

Fig. 2. 2D IR spectra to show intercavity nonlinear interactions between polaritons. (**A**) 2D IR of $W(CO)_6$/hexane in coupled dual cavity. Cross-peaks between polaritons from different cavities are observed (in shaded green areas). The 2D IR peaks that are solely from cavity A are at the corner of blue square and that of cavity B are at the corners of black square. The spectrum was taken with the IR incidence angle (the angle between IR beam and the cavity plane normal, Φ, as shown in fig. S1) to be 11.3°. (**B**) Pump spectral cuts of 2D IR in (A) at $\omega_{pump} = \omega_{UP1}$ (blue), ω_{UP2} (red), ω_{LP1} (yellow), and ω_{LP2} (purple) also show cross-peak features. The green and black arrows in (B) to (E) highlight the cross-peaks due to intercavity nonlinear interactions. (**C** and **D**) Experimental (blue dots) and simulated (yellow) spectral cut at $\omega_{pump} = \omega_{UP1}$ and at $\omega_{pump} = \omega_{UP2}$ and the corresponding simulated contributions from cavities A (purple) and B (green). (**E**) Experimental (blue dots) spectral cut at $\omega_{pump} = \omega_{UP1}$ and simulated cut spectrum with nonlinearity off (sky blue), with delocalization off (red), and delocalization and molecular nonlinearity together (yellow). (**F**) 2D IR dynamics at $\omega_{pump} = \omega_{UP1}$.

the basis of knowledge from previous publications (*4*, *6*–*8*, *21*), we focus on analyzing 2D IR signal at t_2 that is longer than polariton lifetime, e.g., t_2 = 20 ps, where the physics is well understood: The source of nonlinear signals is a nonequilibrium population of dark states of the $W(CO)_6$ asymmetric modes in the cavities. At the long-time limit, polaritons decay and excite dark modes, leading to the derivative signals near UP due to Rabi splitting contraction, and overtone absorptions for the strong absorptive feature at the LP side (detailed explanation in section S3.1) (*4*, *7*, *8*).

To quantitatively understand the spectra, we take cuts of the 2D spectra at several ω_{pump}, corresponding to pump-probe spectra by exciting specific polariton states, and simulate them using model 2 where the absorptive coefficients of molecules are altered by the pump-induced population change in both cavities (see Methods and section S2.3 for details). Figure 2C (a spectral cut at $\omega_{pump} = \omega_{UP1} = 2010\ cm^{-1}$) shows that the simulated spectra match with the experimental results very well, capturing the derivative features on the UP side and the double absorptive features on the LP side (simulations of other spectral cuts are in section S3.2). The only mismatch is a small positive feature near 1940 cm^{-1}, which could be due to higher order excited state absorptions of the reservoir mode—a term that was not included in the simulation.

Further physical insights of the intercavity nonlinear signal are obtained by decomposing the simulated spectra into contributions from cavities A and B. A representative result shows that both the cross-peaks of the spectral cut at UP1 of cavity A—a noticeable derivative feature near $\omega_{probe} = 1995\ cm^{-1}$ and a large absorptive peak at $\omega_{probe} = 1955\ cm^{-1}$ are derived from the nonlinear responses from cavity B (the green trace in Fig. 2C). In contrast, the nonlinear signal of cavity A shows a tiny peak at $\omega_{probe} = 1995\ cm^{-1}$ (the purple trace in Fig. 2C). Because this spectral cut is obtained by pumping UP1 of cavity A, it confirms that exciting cavity A can affect polaritons in cavity B—a nonlinear interaction delocalized between cavities (similar results are shown when pumping LP1 in fig. S4A).

Because the simulation shows that it is necessary to change the reservoir ground and excited state population in both cavities to reproduce the experimental results (simulation based on eq. S18 in section S2.3 and see simulation results in table S1), it suggests that the changes of reservoir population lead to the observed nonlinear signals. Thus, the source of intercavity nonlinear interaction is polariton-reservoir mode interactions [similar to those observed in exciton polaritons (*26*)]: The excited polaritons in cavity A relax to dark reservoir modes, a portion of which is shared with cavity B. The shared excited reservoir modes reduce the Rabi splitting of polaritons in cavity B and introduce absorptions of the excited dark modes, thereby generating nonlinear signals.

We note that such a nonlinear interaction is not detected in spectral cuts of exciting UP2 (Fig. 2D) or LP2 (fig. S4B), as the cavity B contribution can well simulate these spectral cuts. Further study on the 2D IR spectra suggest that the intercavity interaction cross-peaks are highly sensitive to the incident angle (section S3.6): At certain angle, the interactions are mutual between two cavities, i.e., cross-peaks exist when either cavity is excited; whereas at other angles, interactions are optimized in one direction, i.e., only cross-peaks due to exciting either cavity A or B exist. The angular sensitivity further demonstrates that the intercavity polariton nonlinear interaction is originated from photon hopping, which highly depends on beam angles. The physical origin of this dependence is beyond model 2, which warrants momentum imaging experiments and more comprehensive theoretical studies in the future. Without further notification, all 2D IR studies are done at angle = 11.3°, where the cavity A to B interactions are favorable.

Both cavity delocalization and molecular nonlinearity are critical for intercavity polariton nonlinear interactions, as shown by turning off either factor. When delocalization is turned off, a simulated spectrum is similar to the ones of single cavity polaritons (the red trace in Fig. 2E). When molecular nonlinearity is turned off by setting anharmonicity to zero, there are simply no signals (the light blue trace in Fig. 2E).

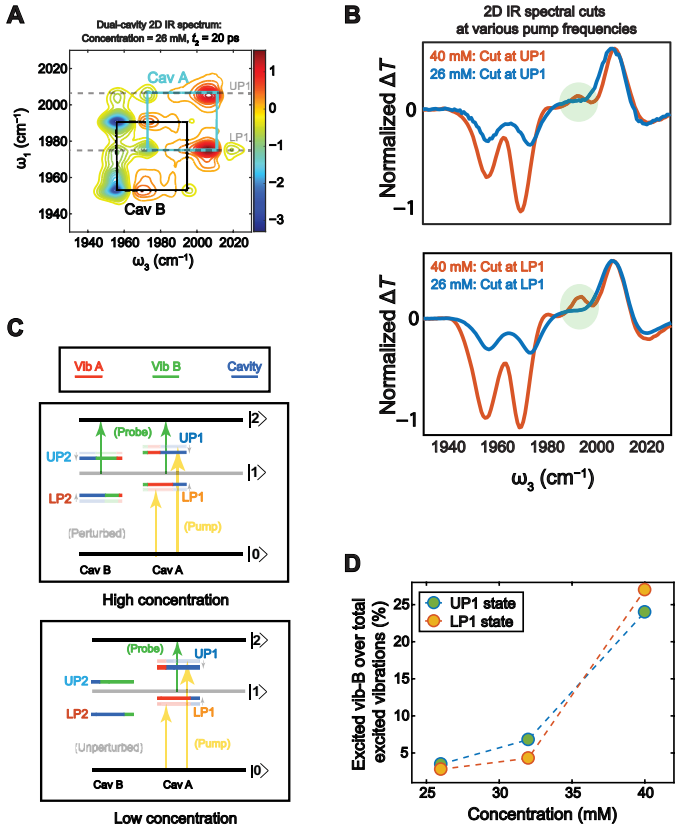

Fig. 3. 2D IR spectrum of dual cavity polaritons at small Rabi splitting. (**A**) 2D IR of $W(CO)_6$/hexane in coupled dual cavity with 26 mM molecular concentration; the 2D IR peaks that are solely from cavity A are at the corner of blue square and that of cavity B are at the corners of black square. (**B**) Pump spectral cuts of 2D IR at $\omega_{pump} = \omega_{UP1}$ and ω_{LP1} (blue/red traces for polariton system with 26/40 mM molecular concentration, both are at $t_2 = 20$ ps) confirm the decrease of cross-peaks with smaller molecular concentration. All data were collected with the incidence IR beam to be 11.3°. (**C**) Schematic illustration of the intercavity coupling enabled/disabled in coupled cavity systems with high/low molecular concentration (top/bottom), |0>, |1>, |2> are the ground, first, and second excited states of the reservoir modes; gray levels indicate the modes are optically dark. (**D**) Percentage of excited vib-B among the total excited vibrational modes in cavity A as a function of molecular concentration, extracted from the spectral fitting results.

The crucial roles of cavity delocalization and molecular nonlinearity can be viewed from the theoretical aspect. In the polariton system, the nonlinear interactions are a result of molecular anharmonicity, which can be written as

$$H_{\text{int}} = Va^{+}a^{+}aa = V\sum_{k_1,k_2,k_3,k_4}^{\text{UP1,UP2,LP1,LP2}} c_{k_1}^{*}c_{k_2}^{*}c_{k_3}c_{k_4}a_{k_1}^{+}a_{k_2}^{+}a_{k_3}a_{k_4} \quad (2)$$

H_{int} is the interaction term of the full polariton Hamiltonian (*4*), where a^{+} and a are the creation and annihilation operators of the molecular vibrational modes in a cavity, and the interaction is local. To derive the second part of the equation, we rewrite $a^{+} = c_{\text{UP1}}^{*}a_{\text{UP1}}^{+} + c_{\text{LP1}}^{*}a_{\text{LP1}}^{+} + c_{\text{UP2}}^{*}a_{\text{UP2}}^{+} + c_{\text{LP2}}^{*}a_{\text{LP2}}^{+}$, where c can be derived from Hopfield coefficient. Terms like $|c_{\text{LP1}}|^{2}|c_{\text{UP2}}|^{2}a_{\text{LP1}}^{+}a_{\text{LP1}}a_{\text{UP2}}^{+}a_{\text{UP2}}$ exist in the second part of Eq. 2, which leads to the nonlinear interaction between LP1 and UP2. The strength of this intercavity polaritonic

interaction depends on the coefficient $|c_{LP1}|^2|c_{UP2}|^2$ and therefore delocalization. For example, if the molecular modes are localized in cavity A, which makes $c_{UP2} = 0$, such an interaction disappears. It is the strong light-matter coupling and photon hopping that render the local molecular mode a linear combination of polaritons in different cavities and thereby delocalize the nonlinearity.

The role of mixing Hopfield coefficient is verified by manipulating the intercavity polariton nonlinear interactions through changing molecular concentration and thereby the collective coupling strength. Spectral cuts at $\omega_1 = \omega_{UP1}$ and ω_{LP1} (Fig. 3B) suggest that no apparent 2D IR cross-peaks at $\omega_3 = \omega_{UP2}$ at lower concentrations (26 mM; Fig. 3A). The cross-peaks at $\omega_3 = \omega_{LP2}$ still appear, suggesting that the interactivity interaction exists. However, by quantitatively extracting the relative population of excited dark modes in cavity B after polaritons in A being excited, we found that the relative population decreases from 24.0 to 3.5%, as the molecular concentration declines from 40 to 26 mM (Fig. 3D and section S3.3). These results qualitatively agree with the four-by-four Hamiltonian matrix model that describes the coupled cavity polaritons (section S3.4). Lowering the concentration results in fewer shared vibrational modes between the two cavities. As summarized in Fig 3C, large Rabi-splitting leads to that a nonnegligible amount of vibrational modes in cavity B (*vib-B*) participates in the formation of LP1 and UP1 states, and a portion of *vib-A* composes LP2 and UP2. Upon pumping LP1 and UP1, it excites the shared *vib-A* and *vib-B* populations, perturbing the energy levels of LP2 and UP2. With small concentration, such a state mixing between cavities reduces, causing intercavity polariton nonlinear interaction to be weakened. We note that this result also serves as a control experiment to show that the observed cross-peaks are not due to spectral filter effects.

We lastly measure the dynamics of the cross-peaks (Fig. 2F), by scanning the waiting time t_2 of the 2D IR spectra. The spectral cut dynamic around $\omega_1 = \omega_{UP1}$=1995 cm^{-1} (Fig. 2F, 2D IR cut at UP1 in the white dashed box) shows that (ω_{UP1}, ω_{UP2}) cross-peak appears within the polariton lifetime (<3 ps, a similar trend can be observed when cutting at $\omega_1 = \omega_{LP1}$; see section S3.6). This result agrees with the mechanism that the evanescent wave of cavity mode leads to the intercavity polariton nonlinear interactions, because the photon hopping can only happen before it leaks out of the cavity.

DISCUSSION

The intercavity polariton nonlinear interaction is exclusively a result of the joint merits of the evanescent wave of cavity modes and molecular nonlinearity. By combining them, a unique property is created, which does not exist in either mode. Achieving the strong coupling regime, which would be the key to the intercavity nonlinear interactions, depends on the selection of molecular and the photonic systems. Overall, the coupling strength (energy exchange rate between matters and photons) should be larger than the spectral linewidth (coherent lifetime) of either mode. Thus, for molecules that have broader linewidth (shorter lifetime), methods that can strengthen coupling, such as enhanced electric fields or higher concentration, are helpful to achieve strong coupling. Once the strong coupling condition is fulfilled, this demonstration could enable polaritonic photonic circuitry in the molecular fingerprint IR regime for low-concentration, compact chemical sensing. The micron-range nonlinear interaction can be further extended to even longer distances when combined with polariton propagation. This experiment also lays a foundation for remote chemistry (*27*), enabling chemistry in one cavity by manipulation of molecules (e.g., as catalysts) in the other cavity. By selectively pumping using a pulse shaper (*28*), the coupled cavity can be an advanced platform for entangled polaritonic qubits.

METHODS

Fabrication of coupled cavity optical mirror

To generate two cavity modes with specific frequency, two different path lengths need to be achieved within one pair of cavity mirrors. A checkerboard pattern is designed and fabricated on the CaF_2 window using photolithography, followed by sputtering deposition of a layer of ZnO and lift-off of ZnO deposited on photoresist, thus leaving behind a checkerboard patterned layer of ZnO on CaF_2. Dielectric coatings (Thin Film Corp.) are deposited on both the flat CaF_2 window and the CaF_2 window with patterned ZnO layer to obtain ~96% reflectivity at around 5-μm wavelength. In this work, a dielectric-coated flat CaF_2 and a dielectric-coated CaF_2 with patterned ZnO (~200-nm thickness) are used in tandem to generate dual cavity modes separated by ~30 cm^{-1} at 5 μm. The frequency separation between the two cavity modes can be tuned by controlling the thickness of the ZnO layer.

Sample preparation

The $W(CO)_6$ (Sigma-Aldrich)/coupled cavity system is prepared in an IR spectral cell (Harrick) containing one flat dielectric CaF_2 mirror and one checkerboard-patterned dielectric CaF_2 mirror, separated by a 12.5-μm Teflon spacer and filled with $W(CO)_6$/hexane solution with various concentrations [40 (saturated concentration), 32, and 26 mM]. The regular $W(CO)_6$/cavity system is prepared in the same way in an IR spectral cell with two flat dielectric CaF_2 mirrors. The cavity mode finesse is around 14 with $\lambda_{FSR}/\Delta\lambda_c$, where λ_{FSR} is the free spectral range and $\Delta\lambda_c$ is the full width at half maximum of the resonance.

2D IR spectroscopy

2D IR spectroscopy (*23*) is applied to investigate the light-matter interaction of a $W(CO)_6$/microcavity system (detailed 2D IR setup and data acquisition are described in section S1.2). Briefly, a pump-probe geometry is adopted where three IR pulses (Fig. 1A) interact with sample systems. The first IR pump pulse and probe pulse generate two coherent states in the system in t_1 and t_3, respectively, which will later be Fourier transformed to the frequency domain as ω_1 (pump frequency) and ω_3 (probe frequency). The second IR pump pulse puts the system in a population state during t_2. All 2D IR spectra in this work are taken at t_2 = 20 ps to avoid interference between pump and probe pulses.

SUPPLEMENTARY MATERIALS

Supplementary material for this article is available at http://advances.sciencemag.org/cgi/content/full/7/19/eabf6397/DC1

REFERENCES AND NOTES

1. O. Wada, Femtosecond all-optical devices for ultrafast communication and signal processing. *New J. Phys.* **6**, 183 (2004).
2. D. Ballarini, M. De Giorgi, E. Cancellieri, R. Houdré, E. Giacobino, R. Cingolani, A. Bramati, G. Gigli, D. Sanvitto, All-optical polariton transistor. *Nat. Commun.* **4**, 1778 (2013).
3. B. S. Simpkins, K. P. Fears, W. J. Dressick, B. T. Spann, A. D. Dunkelberger, J. C. Owrutsky, Spanning strong to weak normal mode coupling between vibrational and Fabry-Pérot

cavity modes through tuning of vibrational absorption strength. *ACS Photonics* **2**, 1460–1467 (2015).
4. R. F. Ribeiro, A. D. Dunkelberger, B. Xiang, W. Xiong, B. S. Simpkins, J. C. Owrutsky, J. Yuen-Zhou, Theory for nonlinear spectroscopy of vibrational polaritons. *J. Phys. Chem. Lett.* **9**, 3766–3771 (2018).
5. K. D. Heylman, K. A. Knapper, R. H. Goldsmith, Photothermal microscopy of nonluminescent single particles enabled by optical microresonators. *J. Phys. Chem. Lett.* **5**, 1917–1923 (2014).
6. A. D. Dunkelberger, R. B. Davidson II, W. Ahn, B. S. Simpkins, J. C. Owrutsky, Ultrafast transmission modulation and recovery via vibrational strong coupling. *J. Phys. Chem. A* **122**, 965–971 (2018).
7. B. Xiang, R. F. Ribeiro, A. D. Dunkelberger, J. Wang, Y. Li, B. S. Simpkins, J. C. Owrutsky, J. Yuen-Zhou, W. Xiong, Two-dimensional infrared spectroscopy of vibrational polaritons. *Proc. Natl. Acad. Sci. U.S.A.* **115**, 4845–4850 (2018).
8. A. D. Dunkelberger, B. T. Spann, K. P. Fears, B. S. Simpkins, J. C. Owrutsky, Modified relaxation dynamics and coherent energy exchange in coupled vibration-cavity polaritons. *Nat. Commun.* **7**, 13504 (2016).
9. X. Liu, T. Galfsky, Z. Sun, F. Xia, E.-c. Lin, Y.-H. Lee, S. Kéna-Cohen, V. M. Menon, Strong light-matter coupling in two-dimensional atomic crystals. *Nat. Photonics* **9**, 30–34 (2014).
10. B. Xiang, R. F. Ribeiro, Y. Li, A. D. Dunkelberger, B. B. Simpkins, J. Yuen-Zhou, W. Xiong, Manipulating optical nonlinearities of molecular polaritons by delocalization. *Sci. Adv.* **5**, eaax5196 (2019).
11. K. E. Dorfman, S. Mukamel, Multidimensional photon correlation spectroscopy of cavity polaritons. *Proc. Natl. Acad. Sci. U.S.A.* **115**, 1451–1456 (2018).
12. M. Stührenberg, B. Munkhbat, D. G. Baranov, J. Cuadra, A. B. Yankovich, T. J. Antosiewicz, E. Olsson, T. Shegai, Strong light-matter coupling between plasmons in individual gold bi-pyramids and excitons in mono- and multilayer WSe_2. *Nano Lett.* **18**, 5938–5945 (2018).
13. T. E. Li, H.-T. Chen, A. Nitzan, J. E. Subotnik, Quasiclassical modeling of cavity quantum electrodynamics. *Phys. Rev. A* **101**, 033831 (2020).
14. B. Xiang, R. F. Ribeiro, M. Du, L. Chen, Z. Yang, J. Wang, J. Yuen-Zhou, W. Xiong, Intermolecular vibrational energy transfer enabled by microcavity strong light–matter coupling. *Science* **368**, 665–667 (2020).
15. A. Thomas, L. Lethuillier-Karl, K. Nagarajan, R. M. A. Vergauwe, J. George, T. Chervy, A. Shalabney, E. Devaux, C. Genet, J. Moran, T. W. Ebbesen, Tilting a ground-state reactivity landscape by vibrational strong coupling. *Science* **363**, 615–619 (2019).
16. M. J. Hartmann, F. G. S. L. Brandão, M. B. Plenio, Strongly interacting polaritons in coupled arrays of cavities. *Nat. Phys.* **2**, 849–855 (2006).
17. S. R. K. Rodriguez, A. Amo, I. Sagnes, L. Le Gratiet, E. Galopin, A. Lemaître, J. Bloch, Interaction-induced hopping phase in driven-dissipative coupled photonic microcavities. *Nat. Commun.* **7**, 11887 (2016).
18. S. Kim, Y. G. Rubo, T. C. H. Liew, S. Brodbeck, C. Schneider, S. Höfling, H. Deng, Emergence of microfrequency comb via limit cycles in dissipatively coupled condensates. *Phys. Rev. B* **101**, 085302 (2020).
19. G. Khitrova, H. M. Gibbs, F. Jahnke, M. Kira, S. W. Koch, Nonlinear optics of normal-mode-coupling semiconductor microcavities. *Rev. Mod. Phys.* **71**, 1591–1639 (1999).
20. Z. Gu, S. Liu, S. Sun, K. Wang, Q. Lyu, S. Xiao, Q. Song, Photon hopping and nanowire based hybrid plasmonic waveguide and ring-resonator. *Sci. Rep.* **5**, 9171 (2015).
21. B. Xiang, R. F. Ribeiro, L. Chen, J. Wang, M. Du, J. Yuen-Zhou, W. Xiong, State-selective polariton to dark state relaxation dynamics. *J. Phys. Chem. A* **123**, 5918–5927 (2019).
22. P. Saurabh, S. Mukamel, Two-dimensional infrared spectroscopy of vibrational polaritons of molecules in an optical cavity. *J. Chem. Phys.* **144**, 124115 (2016).
23. P. Hamm, M. Zanni, *Concepts and Methods of 2D Infrared Spectroscopy* (Cambridge Univ. Press, Cambridge, 2011), vol. 9781107000.
24. J. A. Fournier, W. B. Carpenter, N. H. C. Lewis, A. Tokmakoff, Broadband 2D IR spectroscopy reveals dominant asymmetric $H_5O_2^+$ proton hydration structures in acid solutions. *Nat. Chem.* **10**, 932–937 (2018).
25. D. V. Kurochkin, S. R. G. Naraharisetty, I. V. Rubtsov, A relaxation-assisted 2D IR spectroscopy method. *Proc. Natl. Acad. Sci. U.S.A.* **104**, 14209–14214 (2007).
26. T. Yagafarov, D. Sannikov, A. Zasedatelev, K. Georgiou, A. Baranikov, O. Kyriienko, I. Shelykh, L. Gai, Z. Shen, D. Lidzey, P. Lagoudakis, Mechanisms of blueshifts in organic polariton condensates. *Commun. Phys.* **3**, 18 (2020).
27. M. Du, R. F. Ribeiro, J. Yuen-Zhou, Remote control of chemistry in optical cavities. *Chem* **5**, 1167–1181 (2019).
28. Z. Yang, B. Xiang, W. Xiong, Controlling quantum pathways in molecular vibrational polaritons. *ACS Photonics* **7**, 919–924 (2020).

Acknowledgments: We thank J. Yuen-Zhou and R. F. Ribeiro's constructive feedback to this work. **Funding:** This work is supported by NSF CAREER Award DMR1848215. The fabrication of dual-cavity mirrors was performed in part at the San Diego Nanotechnology Infrastructure (SDNI) of UCSD, a member of the National Nanotechnology Coordinated Infrastructure, which is supported by the NSF (grant ECCS-1542148). B.X. is supported by a Roger Tsien Fellowship from the Department of Chemistry and Biochemistry at UC San Diego. **Author contributions:** W.X. conceived the original idea and developed the theoretical model for linear and nonlinear spectroscopy in this work. J.W. design and fabricated the coupled cavity mirrors. J.W. and B.X. conducted 2D IR experiments, analyzed the data, and performed simulations. Z.Y. contributed to data analysis. J.W., B.X., and W.X. wrote the manuscript. **Competing interests:** The authors declare that they have no competing interests. **Data and materials availability:** All data needed to evaluate the conclusions in the paper are present in the paper and/or the Supplementary Materials. Additional data related to this paper may be requested from the authors.

Submitted 9 November 2020
Accepted 19 March 2021
Published 7 May 2021
10.1126/sciadv.abf6397

Citation: B. Xiang, J. Wang, Z. Yang, W. Xiong, Nonlinear infrared polaritonic interaction between cavities mediated by molecular vibrations at ultrafast time scale. *Sci. Adv.* **7**, eabf6397 (2021).